Check for updates



**Lingyu Wang**
**David Da Yong Chen**

Department of Chemistry, University of British Columbia, Vancouver, BC, Canada

Received May 29, 2019
Revised July 17, 2019
Accepted August 9, 2019

Research Article

# Analysis of four therapeutic monoclonal antibodies by online capillary isoelectric focusing directly coupled to quadrupole time-of-flight mass spectrometry

Capillary isoelectric focusing (cIEF) was online coupled to a Q-TOF MS by a flow-through microvial interface for the analysis of therapeutic mAb. Intact molecular weights obtained from the mass spectrum deconvolution of separated charge variants provided information on the structural heterogeneity of therapeutic mAbs. A sandwich cIEF–MS configuration composed of anolyte, sample, and catholyte segments sequentially injected into a neutrally coated capillary was used for the charge heterogeneity separation of four mAbs. Acetic acid and ammonium hydroxide were used in places of the non-volatile acids and bases commonly used for IEF but are incompatible with online MS detection. Glycerol was added as the anti-convective reagent. A chemical modifier was mixed with the cIEF effluent in the flow-throw microvial to maintain the ESI stability and to mitigate ion suppression from the co-eluted carrier ampholytes and glycerol. Analysis of mAb samples have shown relative populations of two basic variants originating from C-terminal lysine process and acidic variant of deamidation. The lysine clippings, deamidation, and sialic acid modification in oligosaccharide chains were revealed in infliximab. Two lysine clipping variants and a deamidated variant were observed in adalimumab. The duplicate analyses of a reference mAb demonstrated five charge variants separated by cIEF due to some unidentified modifications, as their mass spectra shared close similarities. The mAb analyses demonstrated the feasibility of the cIEF–MS method, and they demonstrated how charge and structural variants and minor differences in therapeutic mAbs are observed with this technology. Online cIEF–MS is an information rich technology with high throughput, demonstrated by the initial data presented here.

**Keywords:**
Capillary isoelectric focusing / Charge heterogeneity / Mass spectrometry / Monoclonal antibodies
DOI 10.1002/elps.201900195

Additional supporting information may be found online in the Supporting Information section at the end of the article.

## 1 Introduction

Antibodies, also known as immunoglobulins (Ig), are secreted and utilized by mammalian immune systems to neutralize detrimental pathogens to maintain health, because their highly selective binding sites target the epitopes of invading viruses, bacteria, fungi, etc. [1]. The Ab paratopes responsible for antigen bindings are determined by the amino acid sequence and structure of the complementarity determining regions. Immunoglobulin G is one of the most important types of Abs in the biopharmaceutical industry [1, 2]. In 2017, five out of ten globally best-selling drugs were monoclonal antibodies. Unlike those small medicinal molecules, the production of therapeutic recombinant mAbs relies on complex protein expression processes by genetically engineered hybridoma cell lines [3]. The mAb production by non-human cell lines, such as CHO, murine NS0, and murine SP2/0, brings non-human amino acid sequences or saccharide residues which may result in risks of immunogenicity [3, 4]. In addition, in vitro mAb modifications introduced during purification, storage, and transportation may also

**Correspondence**: Dr. David D. Y. Chen, Department of Chemistry, University of British Columbia, Vancouver, BC, Canada V6T 1Z1
**E-mail**: chen@chem.ubc.ca

**Abbreviations:** **BPC**, base peak chromatogram; **EIC**, extracted ion chromatogram; **TIC**, total ion chromatograms

**Color online**: See the article online to view Figs. 1–8 in color.

© 2019 WILEY-VCH Verlag GmbH & Co. KGaA, Weinheim

introduce risks of both lowered potency and increased immunogenicity [5].

Most in vitro and in vivo mAb modifications occur alongside shifts in mAb isoelectric point (pI) [6]. Acidic pI shifts may originate from C-terminal lysine clipping, acidic glycan residues in the oligosaccharide chains, glycations on lysines, spontaneous deamidation of asparagine to aspartic acid/isoaspartic acid, etc., while basic pI shifts may be related to N-terminal formation of pyroglutamate from glutamic acid, residual C-terminal lysine, proline/leucine α-amidation, basic amino acid residues in the unremoved leader sequence [4, 7]. In theory, oxidation of methionine and tryptophan, glycosylation heterogeneity because of uncharged saccharide residues, and most cysteine related modifications cannot trigger significant pI changes. Multiple analytical methods are needed for mAb heterogeneity characterization, especially those using orthogonal principles for clone selection and process development [8]. The separation of intact mAb variants (ca. 150 000 Da) with subtle modifications poses challenges on reverse phase liquid chromatography. CZE showed potential in mAb charge variant separation [9]. However, charge heterogeneity analysis relies mainly on specialized methodologies of ion exchange chromatography [10], conventional cIEF [11], and whole column imaging cIEF [12].

IEF has high resolving power for zwitterionic biopolymers because of its focusing-separation principle which can compensate the diffusion of separated analyte zones [13, 14]. A pI difference of 0.003 ΔpH can be resolved by slab-gel IEF with an immobilized pH gradient [15]. Because most discrete IEF peaks of mAb charge variants are approximately spaced with 0.2 ΔpH from each other [16], IEF method development for mAb is usually straightforward. Optical absorbance measurement is the most widely used detection mode for IEF, which provides quantitative information for the assessment of mAb quality and batch-to-batch consistency. Detection mode using native fluorescence generated by tryptophan residues provides higher sensitivity [17]. However, optical detection modes cannot offer any definitive structural information with the IEF traces.

Direct coupling of IEF to MS is attractive because it functions highly similar to 2D gel electrophoresis, while providing faster analyzing time, higher sensitivity, more precise pI values, higher mass accuracy, and powerful MS/MS function [18]. QTOF mass spectrometers are suitable for high mass measurement of intact therapeutic biopolymers, because of the wide mass range and high mass resolution [19]. Offline coupling strategies require eluent fractionation and analyte recovery steps for separated zones from slab IEF, free flow IEF, and preparative cIEF [16, 20, 21]. The first online cIEF–MS method and several following works used an exchange step of the catholyte solution to the CE–MS sheath liquid [22–24]. A sandwich configuration containing the catholyte segment, the sample segment containing analyte and carrier ampholytes, and the anolyte segment in the IEF capillary was used to avoid the exchange step and achieve full automation [25–27]. Direct online cIEF–MS analysis of intact mAbs have been reported using either a stainless-steel flow-through microvial interface [27, 28], or a pulled-glass electrokinetically pumped sheath-flow interface [29]. The reported total ion chromatograms (TIC) containing structural information demonstrated high similarity to imaging IEF traces of identical mAbs [29]. Tryptic peptides [24, 30, 31], IdeS-digested mAb (Cetuximab) [32], intact proteins/mAbs [22, 25–29], and acidic oligosaccharides [33] have been analyzed by direct online cIEF–MS.

With a flow-through microvial interface [34, 35], online cIEF–MS protocols can be established using a sandwich configuration. It has a sample segment located in the middle of the separation capillary and a small basic segment in the capillary distal end serving as the anolyte [27, 28]. To mitigate the diffusion of focused zones and prevent protein precipitation, 20% v/v of glycerol was added [25, 26]. The sandwich configuration was used in this work to analyze four therapeutic mAbs.

## 2 Materials and methods

### 2.1 Chemicals and reagents

Water with 18.2 MΩ·cm resistivity (at 25°C) for preparation of all solutions was freshly obtained from a Milli-Q A10 ultrapure water system (Millipore, Billerica, MA, USA). Acetic acid (>99.9% w/w, LC–MS Grade), formic acid (>99.8% w/w, LC–MS Grade), ammonium hydroxide in water (28% w/w, ACS Grade), methanol (LC–MS Grade), and glycerol (>99% w/w, ACS Grade) were purchased from Sigma Aldrich (Toronto, ON, Canada). Fluka carrier ampholyte (40% w/w in water, pH 3–10), anodic spacer iminodiacetic acid (i.e. the low pH stabilizer, ACS Grade), and cathodic spacer arginine (i.e., the high pH stabilizer, ACS Grade) were obtained from Sigma as well. Five synthetic peptide markers (5 mg/mL in water) with pI 10, 9.5, 7, 5.5, and 4.1 were kindly provided by Sciex Separations (Brea, CA, USA). Commercialized PVA coated capillaries with 50 μm id and 365 μm od were purchased from Agilent Technologies (Santa Clara, CA, USA). An unidentified monoclonal antibody, infliximab (Remicade), and adalimumab (Humira) were kindly provided by Sciex Separations. A standard monoclonal antibody (Reference Material 8671) was purchased from the National Institute of Standards and Technology (NIST, Fort Collins, CO, USA).

### 2.2 Instrumentation

A CESI 8000 Plus CE from Sciex Separations (Brea, CA, USA) was used for cIEF. It was coupled to a TripleTOF 6600 mass spectrometer (Q-TOF MS, Sciex, Concord, ON, Canada) using a flow-through microvial interface [34, 35]. A home-made 3D-adjustable stage was used to hold the ESI sprayer. The ESI voltage was 4.5 kV. A chemical modifier solution was delivered by a Module 11 single channel syringe pump (Harvard Apparatus, Saint-Laurent, QC, Canada). The CE–MS platform was integrated and controlled by the Analyst software

© 2019 WILEY-VCH Verlag GmbH & Co. KGaA, Weinheim 

(Version 1.6.2) from Sciex to achieve full automation. Data processing was performed with Sciex PeakView (Version 1.5) and its Bio Tool Kit algorithm (Version 1.5).

### 2.3 cIEF–MS analysis of intact mAbs

The cIEF catholyte was 1.0% v/v acetic acid (0.175 M, pH 2.75) containing 20% v/v glycerol, and the anolyte was 1.0% w/v ammonia in water (0.587 M, pH 11.51) containing 20% v/v glycerol. mAbs were buffered exchanged to water using 30K cutoff Vivaspin (500 µL) centrifugal concentrators in cases where the mAb was not dissolved in water. The cIEF sample mixture was composed of 0.50 mg/mL mAb sample, 75 µg/mL each for five peptide pI markers, 1.0% w/v Fluka carrier ampholyte (pH 3–10), 2.50 mM arginine, 2.50 mM iminodiacetic acid, and 20% v/v glycerol as the anti-convective reagent. It is noted that the pI markers were not added into the IEF samples of the unidentified mAb and infliximab. The freshly prepared sample mixture was vortexed and then centrifuged for 15 min at 12 000 rpm (9.5 cm rotor radius, 15 000 × g) to remove particulates. A PVA capillary (length 80 cm) served as the separation chamber and it was sequentially injected with catholyte–sample mixture–anolyte, and their length ratio was empirically manipulated to be 4:10:6 based on the injection time under a constant pressure (5 psi), as illustrated in Fig. 1. The chemical modifier was composed of 1.0% v/v formic acid and 80% v/v methanol to facilitate ESI, and its flowrate was 1.0 µL/min during the mobilization stage. In the sample loading and focusing stage, the modifier flowrate was reduced to 0.50 µL/min to minimize the disturbance over IEF inside the capillary.

The effective voltage drop between the capillary inlet and its distal end was 30 kV during the focusing stage and 25.5 kV during the following mobilization stage, as the ESI voltage was 4.5 kV. The focusing process took 25 min. An additional pressure of 0.5 psi was applied on the inlet vial to slightly accelerate the chemical mobilization. During the mobilization stage, the MS Curtain Gas was set to 10 (absolute unit), the interface heater temperature was 150° C, the declustering potential/collisional energy were 80 V/10 V for peptide markers and 180 V/50 V for intact mAbs. The time bins to sum was set as 4 for peptides and 80 for intact mAb, aiming at higher sensitivity for intact biopolymers. In a complete MS microcycle, there was always 1 s for mAb monitoring, and 0.50 s for the detection of peptide markers, if added.

Capillary clean-up was critical to assure the experimental reproducibility. A rinse step with deionized water under 15 psi pressure for 3 to 5 min was immediately applied after each run. When necessary, a rinse step using 3 M urea solution (15 psi for 5 to 10 min) was used to flush out protein residues adsorbed to the inner surface of the neutrally-coated capillary. The neutrally coated capillary was immersed in water during the idle time. PVA coated capillaries demonstrated acceptable analysis reproducibility for up to one week with aforementioned rinse steps.

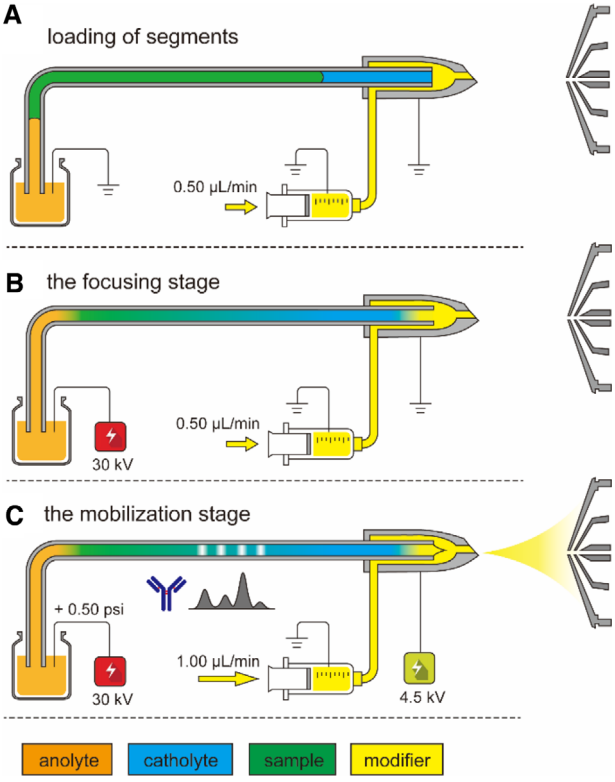



**Figure 1.** Schematics of the online cIEF–MS for a therapeutic mAb sample. The complete analysis includes (A) the sample loading stage, (B) the focusing stage, and (C) the mobilization stage.

## 3 Results and discussion

### 3.1 cIEF–MS analysis of an unidentified mAb

Online cIEF–MS analysis enabled separation of mAb charge variant along with concurrent structural identification for origin of charge heterogeneity. Following our previous study, more types of mAb were subjected to the cIEF–MS analysis to increase the variety of analyte, as a further method proof. First, an unidentified mAb (provided by Sciex Separations) was used on a CE–Q-TOF MS platform. There was a delay in MS acquisition starting time after the cIEF mobilization step to reduce the data file size and avoid part of the MS contamination. A large cohort of ampholyte signal ($m/z$ 300 to 800) was detected during the mobilization stage. Carrier ampholytes with lower pI (longer mobilization time) were detected with higher $m/z$ and the averaged ampholyte $m/z$ value was about 500. Very few ampholyte signals were observed beyond $m/z$ 2000. As shown in Fig. 2A, the stable total ion chromatogram ($m/z$ 1500 to 4000, black trace) demonstrated the ESI stability with the flow-through microvial interface. The volatile chemical modifier was at a high flow rate of 1 µL/min. Because of the noisy background at high $m/z$ range probably due to solvent clusters, the TIC or extracted ion chromatogram did not readily show the IEF separation. However, in the narrow $m/z$ range of 2820 to 2860, the base

© 2019 WILEY-VCH Verlag GmbH & Co. KGaA, Weinheim 

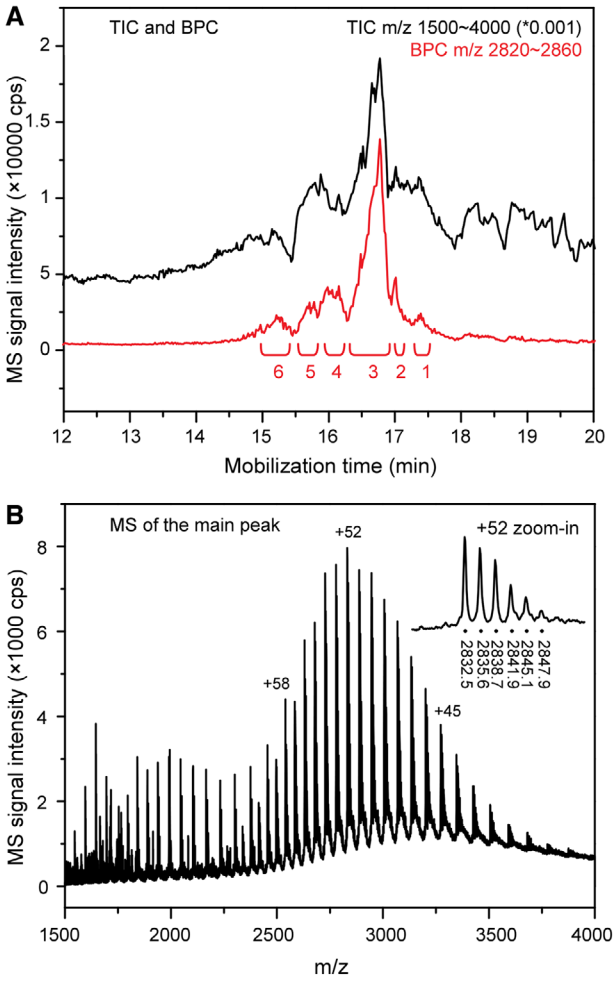



**Figure 2.** (A) cIEF–MS analysis of an unidentified mAb. The total ion chromatograms (TIC) and base peak chromatogram (BPC) demonstrated the IEF separation and ESI stability. For clarity, the intensity of TIC (*m/z* 1500 to 4000) was proportionally reduced by 1000 folds. (B) The averaged mass spectrum of Peak 4 demonstrated the mAb charge envelope. The right zoom-in inset showed the details of the +52 MS peaks for mAb molecules bearing 52 protons.

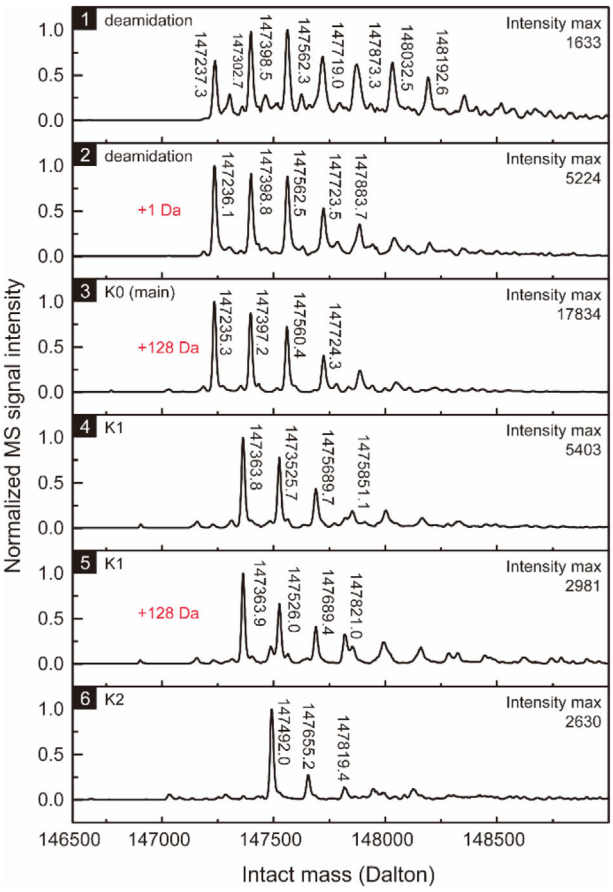



**Figure 3.** Deconvoluted mass spectra of six peaks labeled on the BPC in Fig. 2A. The mass shift of 128 Da between Peak 1 and Peak 2 indicated terminal lysine clipping on the heavy chain, while another 128 Da shift between Peak 3 and Peak 4 is for the second lysine clipping. A 1 Da difference between Peak 4 and Peak 5 indicates a possible deamidated variant, which is confirmed by the acidic pI shift resolved by the IEF separation.

peak chromatogram (BPC) showed six visibly separated peaks in the red trace in Fig. 2A, including the main peak (3), three possible basic variants (4, 5, and 6), and two possible acidic variants (1 and 2). High spectrum quality of the main peak charge envelope demonstrated the feasibility of intact mAb detection even with the interference of background noises originating from both co-eluted carrier ampholytes and solvent clusters containing glycerol. At least five glycoform signals can be clearly defined in the inset of Fig. 2B.

By averaging across six BPC peaks and performing spectrum deconvolutions, the mAb charge envelopes were transformed into a spectrum of intact molecular weight, and the mass shifts between intact weights showed their structural heterogeneity, as shown in Fig. 3. The mass shift of 129.1 ± 0.9 Da ($n = 3$) from Peak 5 to Peak 6, along with the basic pI shift indicated the lysine clipping of K2 to K1 at one of the heavy chain C-terminals [36]. The SD was calculated based on the three most abundant glycoforms. The IEF separation of Peak 4 and Peak 5 was due to unidentified charge heterogeneity, such as a deamidated variant, or simply ESI fluctuation, as their deconvoluted results were similar, with mass shift of ± 0.3 Da. The second C-terminal lysine clipping of K1 to K0 was observed from Peak 3 to Peak 4 with the mass shift of 128.8 ± 0.5 Da, justified by the pI shift towards basic catholyte. The first acidic variant in Peak 2 was proposed to be a deamidated variant, because of the detected small mass shift, 1.5 ± 0.6 Da from the main Peak K0 to Peak 2 [37]. The second acidic variant could not be readily identified by the pI shift and their intact molecule weights, as the three most abundant glycoforms had no significant mass shifts, only 0.2 ± 0.8 Da. Nevertheless, it cannot be simply interpreted as the peak tailing of Peak 2, because two deconvoluted spectra showed obvious compositional differences, including additional minor glycoform peaks (e.g. 147 302.7 Da) and the presence of heavier glycoforms (e.g. 148 032.5 Da). To summarize,

© 2019 WILEY-VCH Verlag GmbH & Co. KGaA, Weinheim

at least four charge variants were unambiguously identified, including the main peak of K0 (Peak 3), two basic charge variants from C-terminal lysine truncation (Peak 4, 5, and Peak 6), and one acidic deamidated variant (Peak 2). Even though fractionation based-methodologies can provide exhaustive interrogation of charge variant species in a therapeutic mAb samples [16], this online cIEF–MS analysis offered a much faster preliminary analysis on charge micro-heterogeneity, as one complete run can be finished within 100 min, including capillary cleaning (<10 min), sample loading (<20 min), focusing (25–30 min), and analyte mobilization and MS detection (30–40 min).

### 3.2 cIEF–MS analysis of infliximab (Remicade)

The cIEF–MS analysis of infliximab showed a TIC plateau peak (2.10–2.90 min) of arginine clusters (i.e. $N \times Arg + H^+$) at the beginning of mobilization as shown in Fig. 4A. The elution of cathodic spacer, which was arginine, signifies the start of the mobilized pH gradient. There were minor fluctuations on the ESI-MS signal, and their amplitude on TIC did not exceed 20% of adjacent signal intensity. Due to the low signal intensity of intact mAb ions and high background noise at the $m/z$ range of 3000 to 4000 as shown in Fig. 4B, there were no clear peaks in the extracted ion chromatograms. However, all charge variants with 48 protons have $m/z$ values within the range of 3000 to 3100. The BPC extracted in this narrower $m/z$ window featured four IEF peaks with sufficient clarity. The highest signal intensity of intact infliximab ions was below 1500 cps, significantly lower than that of unidentified mAb with the same concentration, which was 8000 cps, indicating lowered mAb ionization efficiency. According to the discussion in the supporting information, the lowered ionization efficiency might be due to the intrinsic property of mAb instead of possible MS contamination. The zoomed-in inset demonstrated finer details of the mAb molecules bearing 48 protons, and at least five different glycoforms were detected in one peak cluster.

To investigate the separated BPC peaks to mAb charge and structural heterogeneity, spectrum deconvolution was performed. The deconvoluted mass spectra for four IEF peaks are summarized in Fig. 5. The highest BPC peak, which was defined as the main peak revealed the existence of at least four glycoforms without any terminal lysine residues (i.e. K0), including G0F/G0F, G1F/G0F, and G1F/G1F, which are the most abundant three. Relative to the main peak, the acidic variant demonstrated two noticeable mass shifts. The first one was a 1.1 ± 0.4 Da ($n = 3$) addition, which originated from asparagine deamidation, while the second one noted in Fig. 4A was a 290 Da addition (from 148 845.7–149 135.7 Da), which might indicate the mass shift of one sialic acid (SA, Neu5Ac) addition from 2 × G1F to G1F/G1F(SA). The theoretical mass shift caused by the addition of a terminal Neu5Ac is 291.095 Da [38]. Both the asparagine deamidation and the deletion of the Neu5Ac residue result in acidic pI shifts. It should be emphasized that this was the first time we observed acidic saccharide residues in intact mAb with cIEF–MS analysis. Two basic variants which should originate from C-terminal lysine clippings were well resolved and easily discriminated, with the mass shifts of 128.1 ± 0.2 Da (K1–K0) and 129.7 ± 1.5 Da (K2–K1). The cIEF–MS results were in appropriate accordance with the data reported previously [28, 29]. IEF separation of the deamidated infliximab variant was slightly better than the cIEF–MS method using a pulled-glass interface [29]. The intact mass of the most abundant mAb variant (G0F/G0F, K0) was identical to our previous result [28]. Based on BPCs of two consecutive analyses, the reproducibility was evaluated. It is noted that the baseline for peak integration is shown in Fig. 4A, while the starting and ending times were determined by the characteristics of the deconvoluted mass spectra. For BPC peak K0, K1, and K2, the RSDs were <20%, as listed in Supporting Information Table S1, suggesting the semi-quantitative nature of the cIEF–MS

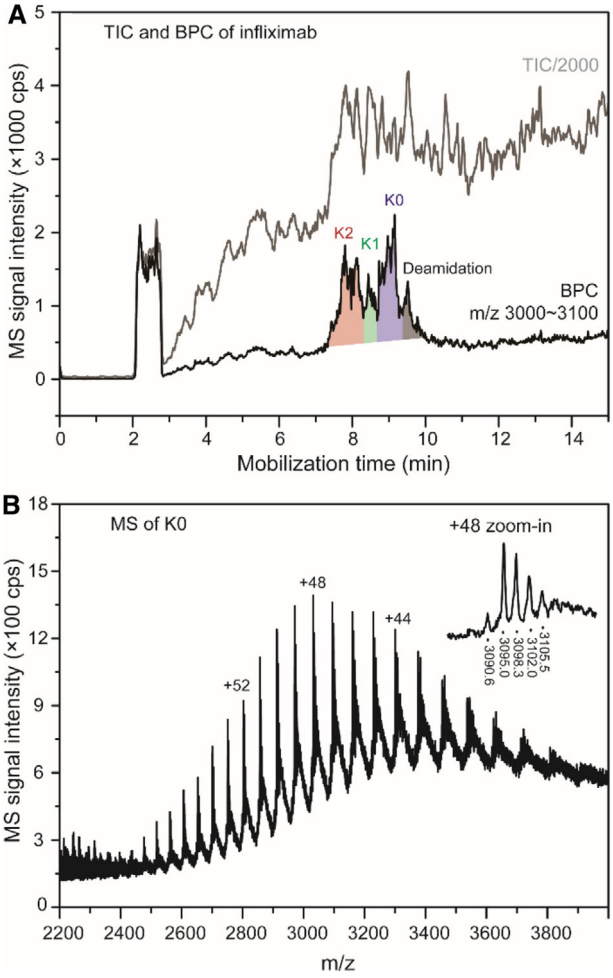



**Figure 4.** (A) TIC and BPC from the cIEF–MS analysis of infliximab. The TIC ($m/z$ 2000 to 4500) intensity was divided by 2000, so that it can be concurrently presented with its BPC ($m/z$ 3000 to 3100). No trace smoothing was applied. (B) The averaged mass spectrum of K0 demonstrated the detection quality of the charge envelope. The right zoom-in inset showed the spectrum details of the +48 mAb molecules bearing 48 protons.

© 2019 WILEY-VCH Verlag GmbH & Co. KGaA, Weinheim 

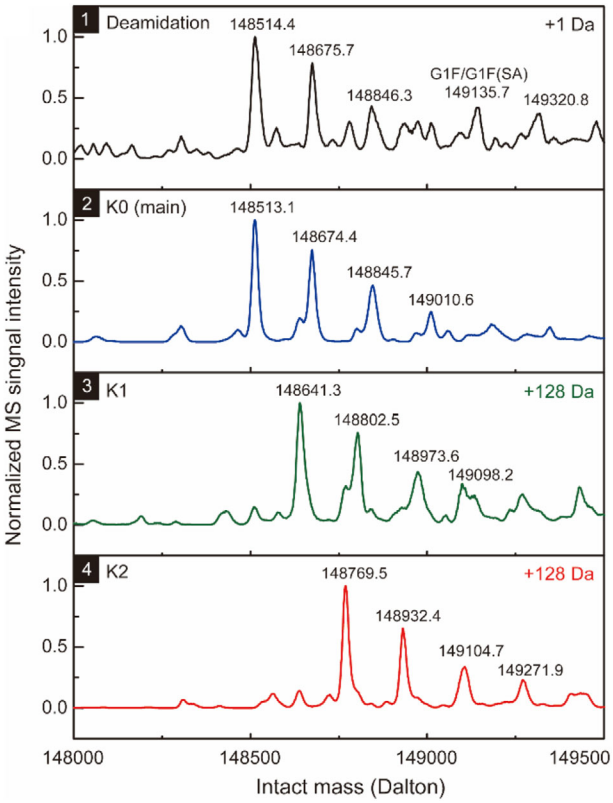



**Figure 5.** Deconvoluted mass spectra of four BPC peaks revealed in Fig. 4A, including (1) one acidic variant of asparagine deamidation, (2) the main peak K0, and (3 and 4) two basic variants of lysing clipping.

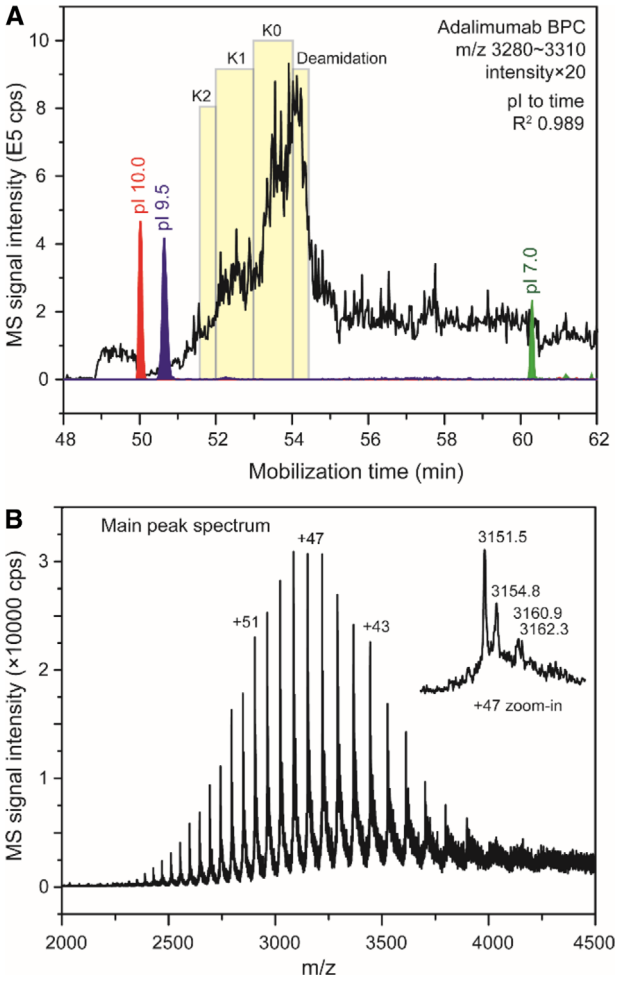



**Figure 6.** (A) The BPC of adalimumab and extracted ion chromatograms of three peptide pI markers in the cIEF–MS analysis. Also shown is the BPC in the *m/z* range of 3280 to 3310 for the peak clusters of mAb + 45 $H^+$ ions. Its intensity was multiplied by 20 and no trace smooth was performed. The *m/z* values of three extracted ion chromatogram traces were 624.330 (pI 10), 950.445 (pI 9.5), and 314.145 (pI 7). The linearity ($R^2$) of markers' pI and migration times was 0.989. (B) The averaged spectrum across the yellow frame K0 in (A) shows the MS spectrum. The zoom-in inset shows the spectrum details of the +47 mAb ions bearing 47 protons.

method. mAb peak area correction using internal standards might decrease the RSD of the integrated peak areas of absolute MS signals.

### 3.3 cIEF–MS analysis of adalimumab (Humira)

The BPC of adalimumab analyses did not produce well-separated peaks, as shown in Fig. 6A. The predominant peak located at around 54 min implies that IEF separation was effective, while the minor peaks for adalimumab charge variants were relatively blurred and could hardly be distinguished from each other on the BPC. In Fig. 5B, the averaged mass spectrum of the main peak showed high signal intensity, but the zoomed-in inset revealed smaller amount of glycoforms in the MS peaks of mAb bearing 47 protons, suggesting the simplicity of adalimumab glycoform cohort. Therefore, another approach of data interrogation was utilized to extract information from those partially separated charge variants. By examining the BPC trace frame by frame, the mobilization time range of focused mAb zones was recognized to be approximately 51.50–54.50 min. To balance the spectrum quality of averaged signals with the temporal resolution of IEF separation, 0.50 min was chosen to be the width of the time slot for spectrum averaging and following deconvolution. In addition, five synthetic peptide pI markers were mixed with the therapeutic mAb, and were concurrently detected by the mass spectrometer swiftly shifting between two detection ranges, *m/z* 300 to 1200 for peptide markers and *m/z* 2000 to 4500 for mAb charge envelopes. The linearity ($R^2$) of pI to migration time was 0.989. In front of the pI 10.0 marker peak, a plateau of arginine clusters was observed. Because of the intense signals of small peptide ions, 66% of the monitoring time was devoted to the intact mAb detection. Based on the mobilization times of pI 9.5 marker and pI 7.0 marker, the pI ranges of six time slots on the BPC was calculated using linear regression. The deconvoluted mass spectra alongside their pI ranges are summarized in Fig. 7.

© 2019 WILEY-VCH Verlag GmbH & Co. KGaA, Weinheim

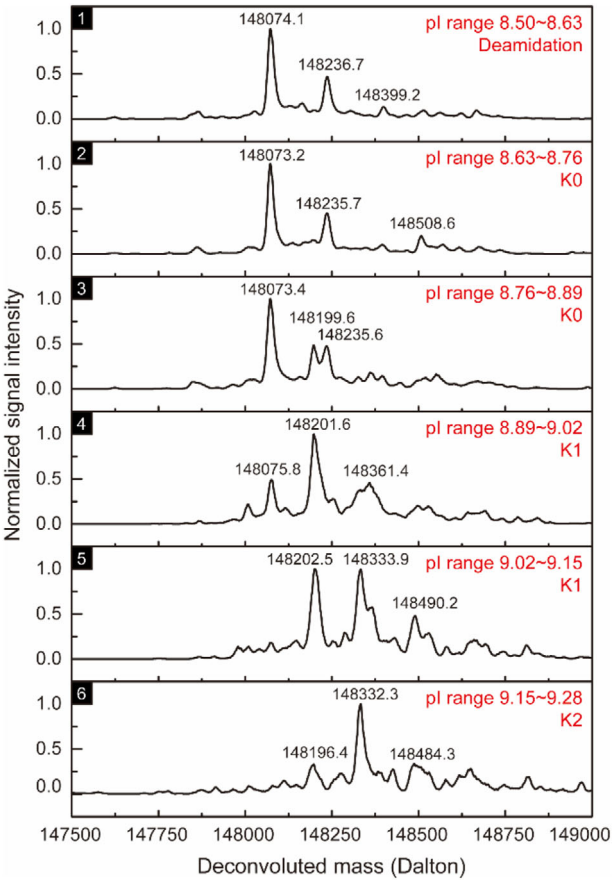



**Figure 7.** Deconvoluted mass spectra of six time slots in the mobilization time range of 51.50–54.50 min of the adalimumab cIEF–MS analysis. For each half-a-minute slot, the corresponding pI range was calculated based on the mobilization times of pI 9.5 marker and pI 7 marker.

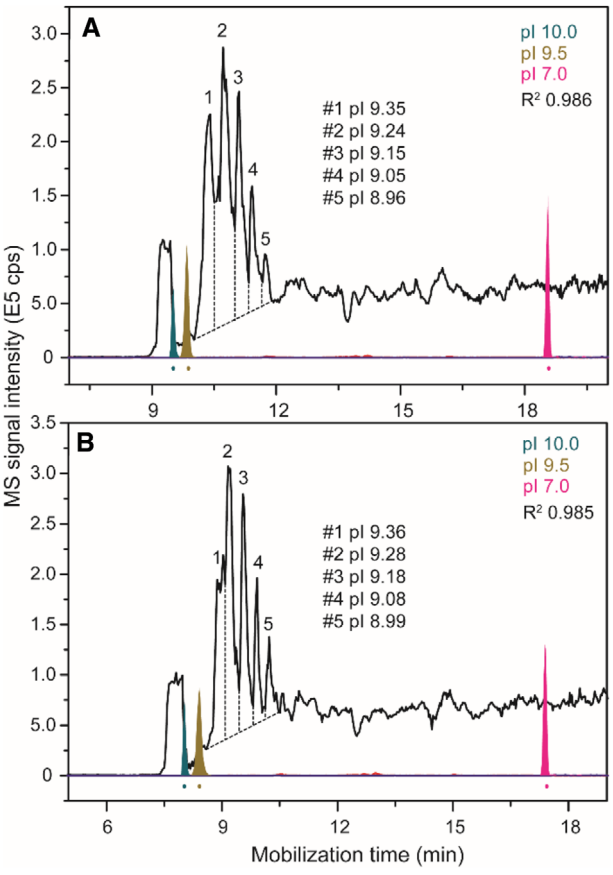



**Figure 8.** The TIC of the NISTmAb and three extracted ion chromatograms of peptide pI markers in the cIEF–MS analysis. (A, B) Duplicate tests had been conducted consecutively in the same day. No trace smooth was performed. The TIC in the *m/z* range of 2000 to 4500 demonstrated five well defined IEF peaks. The *m/z* values of three markers were 624.330 (pI 10), 950.445 (pI 9.5), and 314.145 (pI 7). The linearity ($R^2$) of markers' pI and migration times were 0.986 and 0.985. The pI values of five TIC peaks were calculated based on the migration times of pI 9.5 and 7 markers.

The most basic variant K2, as shown in Fig. 7(6), was detected in the 6$^{th}$ time slot from 51.50 to 52.00 min with the corresponding pI range of 9.15 to 9.28. It showed a mass shift of 129.8 Da relative to the adjacent 5$^{th}$ slot. The second basic variant K1 was found to be located in the 4$^{th}$ and 5$^{th}$ time slots, with a mass shift of 128.7 ± 0.9 Da relative to the 3$^{rd}$ time slot. The main peak K0 was at the 2$^{nd}$ and 3$^{rd}$ time slots with the pI range of 8.63 to 8.89. The lone acidic variant in the pI range of 8.50 to 8.63 resolved by IEF should be a peak for the deamidated form, because it has a 1.0 ± 0.2 Da mass increase relative to the main peak K0. Based on the information extracted from raw mass spectra, the 3-min mAb zone across the TIC can be separated into four regions in which the predominant charge variants can be unambiguously identified. The simultaneous detection of the pI markers provided reliable information for the estimation of charge variant pI values. The measured intact mass for the most abundant adalimumab variant (148 073.2 Da) showed a 10-Da difference relative to the literature value (148 083 Da), which might partially explain the difference between the cIEF–MS profile to the reported cIEF profile [39].

### 3.4 cIEF–MS analysis of NISTmAb (Reference Material 8671)

In the analysis of NISTmAb, we observed high background noise as well, especially in the *m/z* range of 2500 to 4500. Nonetheless, the TICs reproducibly displayed five well-resolved peaks as shown in Fig. 8A and B, unlike analyses of all three other mAb samples which required the extraction of BPCs to display the IEF separation. The first plateau peak on the left-hand side was arginine clusters (i.e. N × Arg + $H^+$). All five numbered peaks in the TICs were deconvoluted for intact molecular weights. It should be noted that the deconvoluted spectrum of Peak 5 was omitted, because it has a vague charge envelope and the corresponding deconvoluted spectrum showed relatively low S/N. Based on the linear regression between migration times and pI values of two adjacent markers, the pI of each TIC peak can be calculated, as listed in Fig. 8A and B. TICs from duplicate tests

© 2019 WILEY-VCH Verlag GmbH & Co. KGaA, Weinheim 

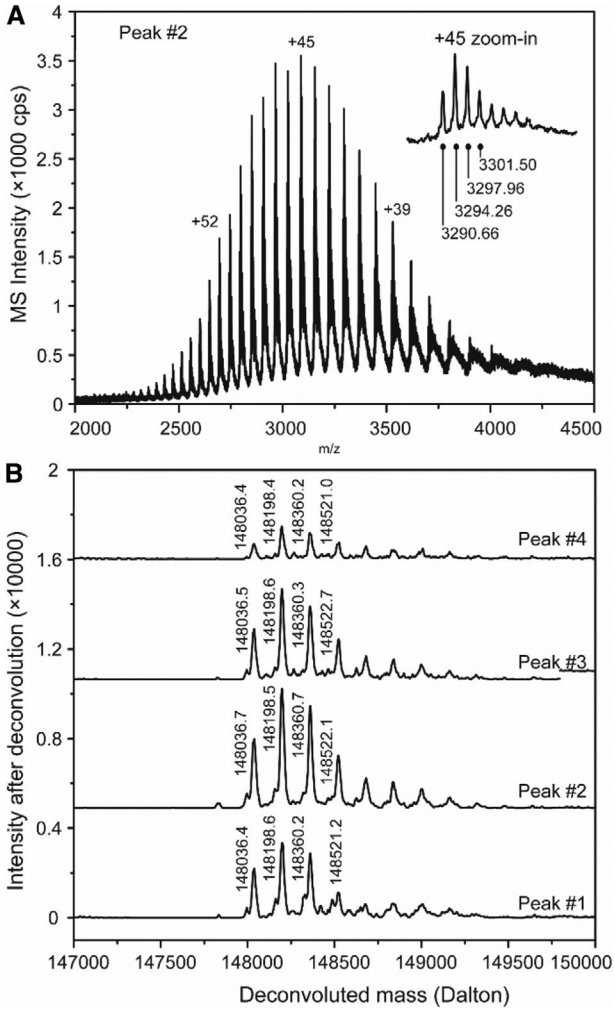



**Figure 9.** (A) The averaged mass spectrum of Peak 2 in Fig. 8 and (B) deconvoluted mass spectra of four TIC peaks. The zoom-in inset demonstrated the MS spectrum details of mAb molecules bearing 45 protons.

showed similar profiles and the calculated values of five peaks demonstrated appropriate consistency, as the biggest pI difference was only 0.04 for Peak 2. The measured NISTmAb pI for the most abundant variant was identical to the literature value measured using imaging cIEF [40]. In addition, the cIEF–MS method showed even better charge variant separation [40]. The RSDs of four TIC peaks were <16%, as listed in Supporting Information Table 1.

The collected mass spectra contained fine details. The zoomed-in inset in Fig. 9A displayed more than seven unique glycoforms bearing 45 protons in Peak 2, indicating the complexity of NISTmAb and the adequate performance of ESI-MS detection. The deconvoluted intact NISTmAb masses were all identical to the theoretical value [41]. The deconvoluted spectra in Fig. 9B showed similar profiles, and we observed neither lysine clipping on heavy chain C-terminals, nor additional sialic acid residues in the oligosaccharide chains. There was a concern that the TIC peaks were formed due to temporal fluctuation of the ESI stability. However, duplicate tests showed reproducible traces and their TICs featured relative smooth baselines with no other peaks besides five mAb isoforms. Therefore, we infer that the IEF separation results may be based on some unknown subtle changes of the protein conformation, such as partial unfolding of the tertiary protein structure. Fractionation after IEF separation and downstream peptide mapping analysis needs to be conducted for structural elucidation of those separated TIC zones.

## 4 Concluding remarks

In this study, we showed the feasibility of an online cIEF–MS method in charge and structural heterogeneity analysis of intact antibodies. Through online assays of four therapeutic mAbs on a CE–QTOF MS platform, we demonstrated fully automated analyses by a sandwich on-capillary configuration. The flow-through microvial interface facilitated the coupling of IEF to online mass spectrometric detection of intact mAb through electrospray ionization. To prevent protein precipitation and avoid extra band broadening, glycerol (20% v/v) was added as the anti-convective additive. A single run required less than 400 ng mAb analyte and less than 100 min, including sample loading, IEF, and chemical mobilization with 0.5 psi extra pressure. Charge variant separation was demonstrated on the TIC or BPC. BPC in a narrow $m/z$ range revealed more well-defined peaks when compared to traces of TIC. Charge variant online identification was achievable because of the intact mAb weights provided by spectrum deconvolution of charge envelopes recorded by the high-resolution Q-TOF MS. The clipping of C-terminal lysines, the asparagine deamidation, and the sialic acid residue in oligosaccharide sidechains on CH2 region had been reproducibly detected. The pI values of well-resolved peaks and focused mAb zones can be calculated based on the mobilization times of co-eluted peptide pI markers. The MS ion suppression was mitigated by the eluent dilution with a high chemical modifier flow rate and the small amount of glycerol and carrier ampholytes used in each analysis. In summary, online cIEF–MS analysis provided a platform to a low time/analyte consumption technique and can be used to separate and identify charge and structural isomers of therapeutic proteins. Further study is in progress, which aims at resolving more acidic variants with low abundances and enhancing the S/N of their charge envelopes.

*This study was supported by Sciex Separations (Brea, CA, USA) and the Natural Sciences and Engineering Research Council of Canada (NSERC). The authors acknowledge help related to instrument operation and data processing from Dr. Fang Wang and Dr. Marcia Santos at Sciex Separations. LW acknowledges the financial support from a 3-year Mitacs Accelerate PhD fellowship sponsored by PromoChrom Technologies, Surrey, BC, Canada.*

*The authors have declared no conflict of interest.*

© 2019 WILEY-VCH Verlag GmbH & Co. KGaA, Weinheim 

## 5 References


[1] Breedveld, F. C., *Lancet* 2000, *355*, 735–740.

[2] Ecker, D. M., Jones, S. D., Levine, H. L., *mAbs* 2015, *7*, 9–14.

[3] Yokoyama, W. M., Christensen, M., Santos, G. D., Miller, D., Ho, J., Wu, T., Dziegelewski, M., Neethling, F. A., *Curr. Protoc. Immunol.* 2006, *102*, 2.5.1–2.5.29.

[4] Liu, H., Ponniah, G., Zhang, H. M., Nowak, C., Neill, A., Gonzalez-Lopez, N., Patel, R., Cheng, G., Kita, A. Z., Andrien, B., *mAbs* 2014, *6*, 1145–1154.

[5] Wang, W., Singh, S., Zeng, D. L., King, K., Nema, S., *J. Pharm. Sci.* 2007, *96*, 1–26.

[6] Vlasak, J., Ionescu, R., *Curr. Pharm. Biotechnol.* 2008, *9*, 468–481.

[7] Liu, H., Gaza-Bulseco, G., Faldu, D., Chumsae, C., Sun, J., *J. Pharm. Sci.* 2008, *97*, 2426–2447.

[8] Schneider, C. K., Vleminckx, C., Gravanis, I., Ehmann, F., Trouvin, J. H., Weise, M., Thirstrup, S., *Nat. Biotechnol.* 2012, *30*, 1179–1185.

[9] Moritz, B., Schnaible, V., Kiessig, S., Heyne, A., Wild, M., Finkler, C., Christians, S., Mueller, K., Zhang, L., Furuya, K., Hassel, M., Hamm, M., Rustandi, R., He, Y., Solano, O. S., Whitmore, C., Park, S. A., Hansen, D., Santos, M., Lies, M., *J. Chromatogr. B* 2015, *983-984*, 101–110.

[10] Rea, J. C., Moreno, G. T., Lou, Y., Farnan, D., *J. Pharm. Biomed. Anal.* 2011, *54*, 317–323.

[11] Salas-Solano, O., Babu, K., Park, S. S., Zhang, X., Zhang, L., Sosic, Z., Boumajny, B., Zeng, M., Cheng, K.-C., Reed-Bogan, A., Cummins-Bitz, S., Michels, D. A., Parker, M., Bonasia, P., Hong, M., Cook, S., Ruesch, M., Lamb, D., Bolyan, D., Kiessig, S., Allender, D., Nunnally, B., *Chromatographia* 2011, *73*, 1137–1144.

[12] Salas-Solano, O., Kennel, B., Park, S. S., Roby, K., Sosic, Z., Boumajny, B., Free, S., Reed-Bogan, A., Michels, D., McElroy, W., Bonasia, P., Hong, M., He, X., Ruesch, M., Moffatt, F., Kiessig, S., Nunnally, B., *J. Sep. Sci.* 2012, *35*, 3124–3129.

[13] Hjerten, S., Zhu, M. D., *J. Chromatogr. A* 1985, *346*, 265–270.

[14] Rodriguez-Diaz, R., Wehr, T., Zhu, M. D., *Electrophoresis* 1997, *18*, 2134–2144.

[15] Cossu, G., Righetti, P. G., *J. Chromatogr. A* 1987, *398*, 211–216.

[16] Hosken, B. D., Li, C., Mullappally, B., Co, C., Zhang, B., *Anal. Chem.* 2016, *88*, 5662–5669.

[17] Lillard, S. J., Yeung, E. S., *J. Chromatogr. B* 1996, *687*, 363–369.

[18] Huhner, J., Lammerhofer, M., Neususs, C., *Electrophoresis* 2015, *36*, 2670–2686.

[19] Qu, M., An, B., Shen, S., Zhang, M., Shen, X., Duan, X., Balthasar, J. P., Qu, J., *Mass Spectrom. Rev.* 2017, *36*, 734–754.

[20] Davidsson, P., Folkesson, S., Christiansson, M., Lindbjer, M., Dellheden, B., Blennow, K., Westman-Brinkmalm, A., *Rapid Commun. Mass Spectrom.* 2002, *16*, 2083–2088.

[21] Silvertand, L. H., Torano, J. S., de Jong, G. J., van Bennekom, W. P., *Electrophoresis* 2009, *30*, 1828–1835.

[22] Tang, Q., Harrata, A. K., Lee, C. S., *Anal. Chem.* 1995, *67*, 3515–3519.

[23] Clarke, N. J., Tomlinson, A. J., Naylor, S., *J. Am. Soc. Mass Spectrom.* 1997, *8*, 743–748.

[24] Kuroda, Y., Yukinaga, H., Kitano, M., Noguchi, T., Nemati, M., Shibukawa, A., Nakagawa, T., Matsuzaki, K., *J. Pharm. Biomed. Anal.* 2005, *37*, 423–428.

[25] Mokaddem, M., Gareil, P., Varenne, A., *Electrophoresis* 2009, *30*, 4040–4048.

[26] Lecoeur, M., Gareil, P., Varenne, A., *J. Chromatogr. A* 2010, *1217*, 7293–7301.

[27] Zhong, X., Maxwell, E. J., Ratnayake, C., Mack, S., Chen, D. D., *Anal. Chem.* 2011, *83*, 8748–8755.

[28] Wang, L., Bo, T., Zhang, Z., Wang, G., Tong, W., Da Yong Chen, D., *Anal. Chem.* 2018, *90*, 9495–9503.

[29] Dai, J., Lamp, J., Xia, Q., Zhang, Y., *Anal. Chem.* 2018, *90*, 2246–2254.

[30] Zhu, G., Sun, L., Yang, P., Dovichi, N. J., *Anal. Chim. Acta* 2012, *750*, 207–211.

[31] Zhu, G., Sun, L., Keithley, R. B., Dovichi, N. J., *Anal. Chem.* 2013, *85*, 7221–7229.

[32] Dai, J., Zhang, Y., *Anal. Chem.* 2018, *90*, 14527–14534.

[33] Ouyang, Y., Han, X., Xia, Q., Chen, J., Velagapudi, S., Xia, K., Zhang, Z., Linhardt, R. J., *Anal. Chem.* 2019, *91*, 846–853.

[34] Maxwell, E. J., Zhong, X., Zhang, H., van Zeijl, N., Chen, D. D., *Electrophoresis* 2010, *31*, 1130–1137.

[35] Zhong, X., Maxwell, E. J., Chen, D. D., *Anal. Chem.* 2011, *83*, 4916–4923.

[36] Antes, B., Amon, S., Rizzi, A., Wiederkum, S., Kainer, M., Szolar, O., Fido, M., Kircheis, R., Nechansky, A., *J. Chromatogr. B* 2007, *852*, 250–256.

[37] Huang, L., Lu, J., Wroblewski, V. J., Beals, J. M., Riggin, R. M., *Anal. Chem.* 2005, *77*, 1432–1439.

[38] Varki, A., *Trends Mol. Med.* 2008, *14*, 351–360.

[39] Liu, J., Eris, T., Li, C., Cao, S., Kuhns, S., *BioDrugs* 2016, *30*, 321–338.

[40] Goyon, A., Excoffier, M., Janin-Bussat, M.-C., Bobaly, B., Fekete, S., Guillarme, D., Beck, A., *J. Chromatogr. B* 2017, *1065-1066*, 119–128.

[41] Formolo, T., Ly, M., Levy, M., Kilpatrick, L., Lute, S., Phinney, K., Marzilli, L., Brorson, K., Boyne, M., Davis, D., Schiel, J., *State-of-the-Art and Emerging Technologies for Therapeutic Monoclonal Antibody Characterization Volume 2. Biopharmaceutical Characterization: The NISTmAb Case Study*, American Chemical Society 2015, pp. 1–62.


© 2019 WILEY-VCH Verlag GmbH & Co. KGaA, Weinheim 